Available online at www.sciencedirect.com
SCIENCE DIRECT®
ELSEVIER
Physica C 404 (2004) 135–139
PHYSICA C
www.elsevier.com/locate/physc

Vortex lattice reorientation and anisotropy in MgB_2 — effects of two-band superconductivity

C.D. Dewhurst [a,*], R. Cubitt [a], M.R. Eskildsen [b,1], J. Jun [c], S.M. Kazakov [c], J. Karpinski [c]

[a] *Institut Laue Langevin, 6 rue Jules Horowitz, 38042 Grenoble, France*
[b] *DPMC, University of Geneva, 24 Quai E. Ansermet, CH-1211 Geneva, Switzerland*
[c] *Solid State Physics Laboratory, ETH, CH-8093 Zurich, Switzerland*

Abstract

We present small-angle neutron scattering (SANS) measurements of the vortex lattice (VL) in single crystal MgB_2 — a two-band superconductor. Bragg diffraction of neutrons visualizes the structure and orientation of the VL while the scattered intensity probes the super-carrier density. Superconductivity in the π-band is rapidly suppressed with increasing field with a corresponding decrease in scattered intensity and a re-orientation of the VL between 0.5 and 0.9 T. Both these observations are consistent with superconductivity in the π-band being weaker than in the σ-band ($\Delta_\pi < \Delta_\sigma$), and a changing influence of different parts of the Fermi surface determining the VL orientation. SANS measurements of the VL for fields applied at an angle to the *c*-axis allow the penetration depth anisotropy, γ_λ, to be estimated.

PACS: 74.25.Qt; 74.70.Ad; 61.12.Ex
Keywords: Small-angle neutron scattering; Vortex lattice; MgB_2

MgB_2 is a relatively new discovery in the family of superconducting materials and has the highest critical temperature, $T_c \approx 39$ K, for a simple binary compound. What makes superconductivity unusual in this compound is the now well established fact that there are two distinct energy gaps associated with different parts of the Fermi surface. The larger gap ($\Delta_\sigma \approx 7$ meV) originates from holelike carriers residing on two cylindrical Fermi surface sheets, derived from σ bonding of the p_{xy} boron orbital (σ-band). The smaller gap ($\Delta_\pi \approx 2$ meV) originates from two 3D sheets of electrons and holes derived from π bonding of the p_z orbitals (π-band) [1–3]. There are, therefore, two different sources of supercarriers, one being almost isotropic (π-band) and the other highly anisotropic (σ-band).

Imaging of the vortex lattice (VL) in MgB_2 has been reported previously using techniques such as STM [4], decoration [5] and small-angle neutron scattering (SANS) [6,7]. STM and decoration

* Corresponding author. Tel.: +33-4-76-20-73-82; fax: +33-4-76-20-71-20.
E-mail address: dewhurst@ill.fr (C.D. Dewhurst).
[1] Current address: Department of Physics, University of Notre Dame, Notre Dame, IN 46556–5670, USA.

0921-4534/$ - see front matter
doi:10.1016/j.physc.2003.09.105

experiments provide a direct, 'real space' image of the vortices but are generally restricted to a few VL unit cells, with STM having the added advantage that tunnelling spectra can be recorded providing information about the (two) energy gap(s) [4,8,9]. Interestingly, measurements of the VL and core size by STM with $B\|c$ show a triangular VL and 'large' vortex cores at low fields associated with an effective $\xi_\pi \approx 500$ Å for the π-band, far greater than $\xi_\sigma \approx 100$ Å deduced from $B_{c2}(0) = 3.1$ T ($B\|c$) [10]. STM also shows that superconductivity of the π-band is suppressed at much lower fields than the σ-band. Hence, at low temperatures the σ-band controls the bulk upper critical field applied parallel to the c-axis [4,9].

It is common place to define the superconducting anisotropy in terms of the magnetic penetration depth, λ, with $\gamma_\lambda = \lambda_c/\lambda_{ab}$, and the upper critical field, B_{c2}, with $\gamma_H = B_{c2\perp c}/B_{c2\|c}$. Usually the two anisotropies are identical, but in a two-band superconductor at low temperatures this need not necessarily be the case [11]. In MgB_2 this is easily seen since λ depends on the total supercarrier density whereas it is primarily the σ-band which is responsible for the upper critical field anisotropy. Calculations predict $\gamma_\lambda = 1$–1.2 and $\gamma_H = 6$ at low temperature, with the two merging at $\gamma_\lambda = \gamma_H = 2.6$ due to thermal mixing between bands for temperatures approaching T_c [11].

In this paper we report SANS measurements of the VL, a bulk measurement where coherent Bragg diffraction from the VL represents a sample average of the VL order, symmetry and alignment of the internal field distribution in 'reciprocal space'. Initial SANS measurements of the VL in MgB_2 on powdered samples could not determine directly the morphology of the VL but did allow, for the first time, an estimate of the penetration depth anisotropy, $\gamma_\lambda \sim 1.4$ (2 K, 0.5 T) [6]. The first work on diffraction from the VL in single crystal MgB_2 is detailed in Ref. [7] and is also the subject of this paper.

Small-angle neutron scattering measurements were carried out using the D22 diffractometer, at the Institut Laue Langevin, Grenoble, France. SANS from the VL has been described in detail elsewhere [6,7]. Briefly, the VL in a type II superconductor produces a modulating magnetic field which can coherently scatter the neutron leading to Bragg peaks. Incident neutrons had a wavelength of $\lambda_n = 10$ Å and wavelength spread of $\Delta\lambda_n/\lambda n = 10\%$. The sample and cryomagnet could be titled together about a horizontal or vertical axis to satisfy the Bragg condition for any particular diffraction spot. Background measurements, taken with the sample in the normal state, have been subtracted from each pattern prior to analysis. Most of the results presented here were measured on a 98 μg single crystal platelet with a thickness of 50–100 mm parallel to the c-axis. A second larger crystal with mass 200 μg was also measured. Neutron scattering measurements on crystals of this size is almost unprecedented and is a testament to the short penetration depth of MgB_2 (magnetic contrast) and the high neutron flux available at the ILL. The crystal was grown using isotopically enriched ^{11}B to reduce neutron absorption although contamination of ~7% ^{10}B in the resulting crystal came from the use of a natural BN crucible [12].

Diffraction patterns from the VL measured at 2 K and for fields of 0.5, 0.7 and 0.9 T applied parallel to the c-axis are shown in Fig. 1(a)–(c). Each image is the sum a number of measurements at different angular positions in order to satisfy the Bragg condition for the different peaks. At the lowest field of 0.5 T, Fig. 1(a) shows a sixfold symmetric diffraction pattern with the Bragg peaks oriented along the a-axis of the crystal. This corresponds to a 30° rotation of the real space image with the nearest neighbour (nn) direction perpendicular to the a-axis, as shown schematically in Fig. 2. A hexagonal VL in MgB_2 is expected since the underlying crystal symmetry is also hexagonal. Fig. 1(b) shows that at 0.7 T each of the six peaks have symmetrically split into two. This corresponds to the VL being broken into domains, each one aligned along one of the equivalent directions and mutually rotated by a few degrees relative to the low field orientation. The splitting angle, α, extracted from the data by fitting a two-dimensional Gaussian to each peak, increases with increasing field (Fig. 2) until the two domains orientations have each rotated by 30° to reform a single domain (Fig. 1(c)). At high fields, the VL nn direction is thus aligned parallel to the a-axis.

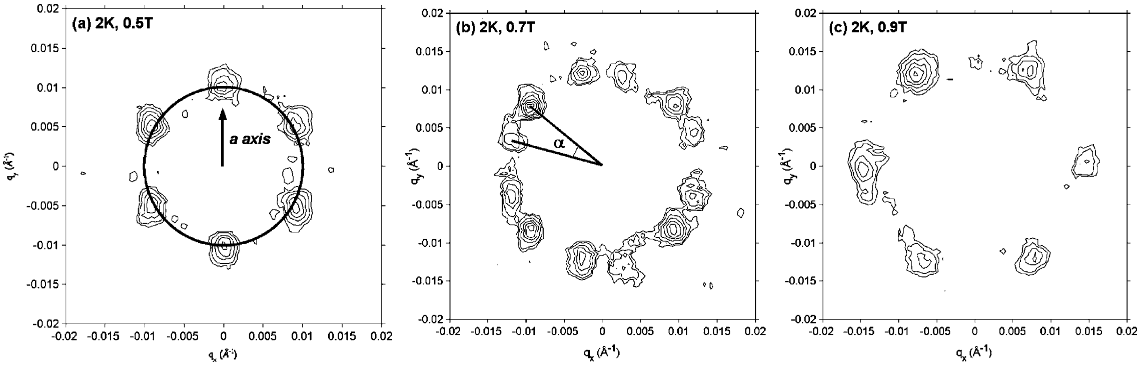

Fig. 1. SANS diffraction patterns from the VL in MgB_2 at 2 K at fields of (a) 0.5 T, (b) 0.7 T and (c) 0.9 T ($B\|c$). The VL splits into two domain orientations of separation angle α, increasing with field until reforming a single rotated domain at high fields (c).

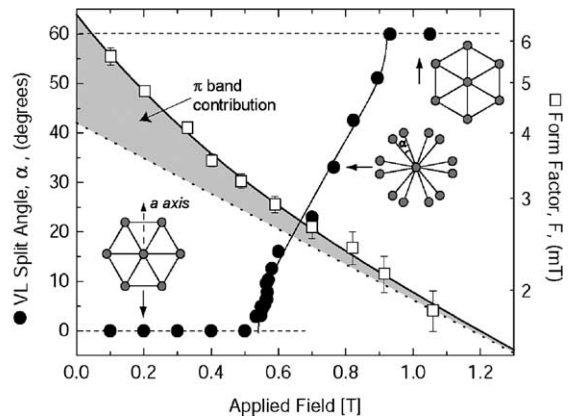

Fig. 2. VL domain split angle, α, vs. field at 2 K. The real space VL orientation is also depicted schematically. The form factor, F, on a log scale, derived from the scattered intensity is fitted as described in the text and in Ref. [7]. The deviation from exponential behaviour (dashed line) at low fields is due to additional supercarriers in the π-band, indicated by the shaded area.

Fig. 2 shows that the abrupt onset of the reorientation occurs at ~0.5 T followed by a continuous increase of α as a function of field up to ~0.9 T.

Also shown in Fig. 2 is the form factor, F, extracted from the integrated intensity of the Bragg peaks. The form factor quantifies the amplitude of the magnetic field modulation in reciprocal space due to the VL [7]. For a conventional single-band superconductor with λ and ξ both independent of field, F, plotted on a logarithmic scale vs. field should yield a straight line. The zero-field value is determined by λ^{-2} and the gradient is proportional to ξ^2. Fig. 2 shows that the data departs significantly from the exponential behaviour expected at low fields. In the London model this is consistent with a loss of supercarrier density, $n_s \propto m^*/\lambda^2$, with increasing field. We associate the loss of supercarrier density with a suppression of the π-band, in agreement with the results from STM [4,8,9]. The fit to the form factor plot shown in Fig. 2 involves a simple model for an exponentially decreasing π-band contribution [7]. The fit yields a characteristic field for the exponential decay of $B^* = 0.3(1)$ T, $\xi_{ab} = 80(10)$ Å, and a π-band weighting of 0.38(14) in reasonable agreement with band structure calculations that suggest 55% of the total zero-field supercarriers come from the π-band [1,2]. The value of B^* agrees well with the upper critical field for the isolated π-band deduced from specific heat measurements [13]. Extrapolating the fit to zero yields an estimate for the zero-field penetration depth, $\lambda_{ab} = 820(20)$ Å, while extrapolating the high-field linear part (dashed line in Fig. 2) to zero yields a second value of $\lambda_{ab} = 1040(100)$ Å, corresponding to the high-field limit where the σ-band dominates the superconductivity.

It is well known that the shape of the Fermi surface and underlying crystal symmetry is 'imprinted' on the superconducting screen currents circulating around vortices and can effect the VL symmetry and orientation with respect to the underlying crystal lattice [14]. Band structure calculations by Kortus et al. [3,15] show the in-plane maximum Fermi velocity directions, $v_{F\_\max}$, reflect the hexagonal crystal symmetry and, crucially, have maximal directions at 30° from each other for the π and σ-bands. The π-band $v_{F\pi\_\max}$ is oriented along the *a*-axis while the σ-band $v_{F\sigma\_\max}$ at 30° from the *a*-axis. When non-local electrodynamics are important the VL the nn direction should be along the Fermi velocity minimum [14]. Thus, our observation of the low field VL oriented with nn at 30° to the *a*-axis is consistent with a dominant π-band. We propose that as the field is increased and superconductivity in the weaker π-band is suppressed the VL gradually rotates to the orientation favoured by the σ-band. However, it is clear from Fig. 2 there are no sharp features in the form factor coinciding with the reorientation onset fields. The reorientation must depend, therefore, on a delicate balance between the free energy of the two orientations.

Rotating the applied field away from the *c*-axis results in a distortion of the VL, due principally to the penetration depth anisotropy, γ_λ. Fig. 3(a) shows the diffraction pattern measured at 2 K in a field 0.4 T applied at 70° to the *c*-axis (*a*-axis remaining vertical). Now the Bragg peaks lie on an ellipse rather than a circle (Fig. 1(a)), since the screening currents must cross the crystallographic basal plane. When λ_c is larger than λ_{ab} ($\gamma_\lambda > 1$), this leads to a stretching of the current loop in the direction of the sample rotation. Campbell et al. [16] described analytically the structure of the VL in an anisotropic uniaxial superconductor for fields at an angle to the principle axes based upon a London approach. They show that the ratio of the major to minor axes of the ellipse connecting the Bragg peaks, ε, is related to the penetration depth anisotropy as:

$$\varepsilon^2 = \left(\frac{\gamma_\lambda^2}{\sin^2 \psi + \gamma_\lambda^2 \cos^2 \psi} \right) \tag{1}$$

where ψ is the angle between the applied field and the *c*-axis. Fig. 3(b) shows ε verses ψ, determined form the fitted Bragg peak positions for measurement angles between 0° and 70°. A fit of Eq. (1) is indicated by the solid line and confirms the applicability of Eq. (1) despite its formulation based on a single-band anisotropic superconductor. The fit yields an anisotropy $\gamma_\lambda = 1.63(6)$ at 2 K and for a field of 0.4 T. It is expected that γ_λ is both field dependent (due to preferential suppression of the π-band) and temperature dependent (due to thermal mixing of the π and σ-bands), and indeed as suggested by our experimental data presented in Ref. [7]. Calculations of the low temperature value of $\gamma_\lambda = 1.1$ [11] do not take into account the field induced suppression of the π-band and this value should therefore be taken as the zero-field limit. Ideally, a measurement of the VL for $B\|a$ would have allowed a direct measurement of γ_λ without the necessity of Eq. (1). Unfortunately measure-

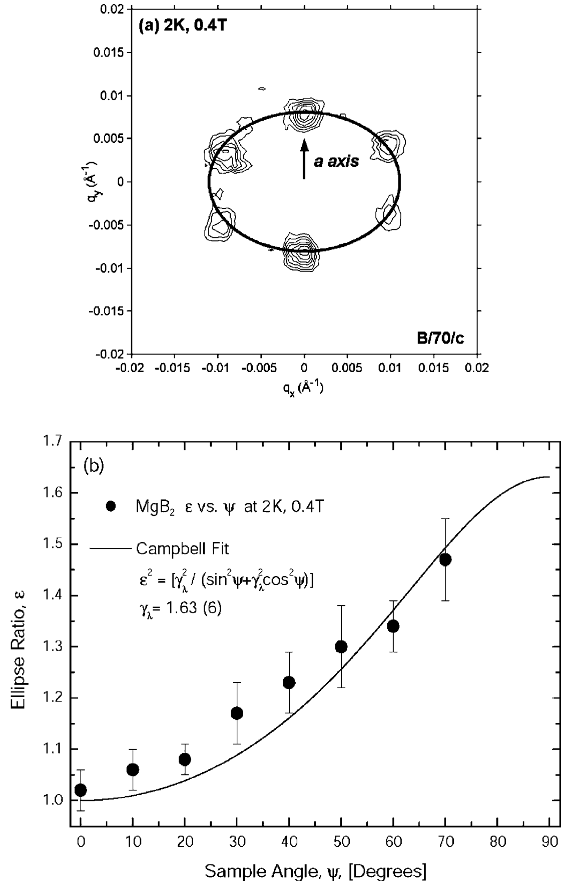

Fig. 3. (a) Anisotropic VL in MgB_2 at 2 K with a field of 0.4 T applied at an angle $\psi = 70°$ to the *c*-axis. The ellipse highlights the positions of the VL Bragg peaks for a fitted ellipse major/minor axis ratio, $\varepsilon = 1.43(3)$ in (a). (b) ε vs. ψ for angles from $\psi = 0$ (i.e. $B\|c$) to $\psi = 70°$. A fit of Eq. (1) (solid line) confirms reasonable agreement with the Campbell model of Ref. [16] yielding a penetration depth anisotropy, $\gamma_\lambda = 1.63(6)$ at 2 K, 0.4 T.

ments at angles greater than 70° were unsuccessful due to the finite ^{10}B content and platelet dimensions of our crystal resulting in significant neutron absorption at high angles.

Finally, we revisit the re-orientation of the VL attributed here and in Ref. [7] to the rapid suppression of the π-band with increasing field. Since the π-band is almost isotropic we might expect that it is suppressed in a similar manner, independent of the field angle to the *c*-axis. Fig. 4 shows the diffraction pattern from the VL in a second (200 μg) MgB_2 single crystal, at 2 K in an applied field of 0.7 T inclined at 70° to the *c*-axis. We find that the VL has undergone a reorientation when compared to Fig. 3(a), analogous to what we found for $B\|c$ (Fig. 1).

In conclusion, we have measured the structure and orientation of the vortex lattice in single crystals of MgB_2 using small-angle neutron scattering. For applied fields parallel to the *c*-axis the VL reorients by 30° between 0.5 and 0.9 T. This is coincident with a loss of scattered intensity attributed to the change in supper carrier density as superconductivity in the weaker π-band is suppressed by the applied field. The VL orientation at low and high fields is likely determined by the Fermi surface anisotropy (via non-local effects) of the π and σ-bands respectively which are thought to exhibit hexagonal symmetries mutually rotated by 30°. Measurements of the VL in fields inclined to the *c*-axis allow the anisotropy of the VL to be measured and an estimate of the penetration depth anisotropy, $\gamma_\lambda = 1.63(6)$ (2 K, 0.4 T), to be made. The validity of Eq. (1) has been established up to angles of $B/70°/c$, despite its application to MgB_2, a two-band superconductor. The reorientation of the vortex lattice is robust up to high angles to the *c*-axis and appears to be a direct manifestation of two-band superconductivity in MgB_2 with differing band properties.

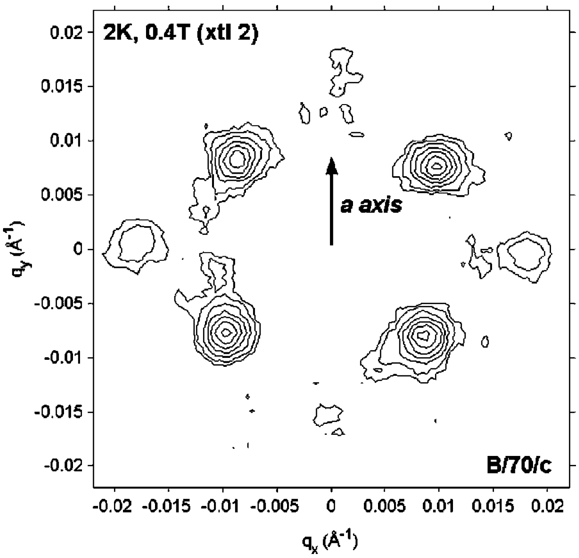

Fig. 4. Anisotropic and re-oriented VL in MgB_2 (crystal 2) at 2 K with a field of 0.7 T applied at an angle $\psi = 70°$ to the *c*-axis.

References

[1] A.Y. Liu, I.I. Mazin, J. Kortus, Phys. Rev. Lett. 87 (2002) 087005.

[2] H.J. Choi, D. Roundy, H. Sun, M. Cohen, S.G. Loule, Nature (London) 418 (2002) 758.

[3] J. Kortus, I.I. Mazin, K.D. Belashchenko, V.P. Antropov, L.L. Boyer, Phy. Rev. Lett. 86 (2002) 4656.

[4] M.R. Eskildsen, M. Kugler, S. Tanaka, J. Jun, S.M. Kazakov, J. Karpinski, Ø. Fischer, Phys. Rev. Lett. 89 (2002) 187003.

[5] L.Ya. Vinnikov, J. Karpinski, S.M. Kazakov, J. Jun, J. Anderegg, S.L. Bud'ko, P.C. Canfield, Phys. Rev. B 67 (2003) 092512.

[6] R. Cubitt, S. Levett, S.L. Bud'ko, N.E. Anderson, P.C. Canfield, Phys. Rev. Lett. 90 (2003) 157002.

[7] R. Cubitt, M.R. Eskildsen, C.D. Dewhurst, J. Jun, S.M. Kazakov, J. Karpinski, Phys. Rev. Lett. 91 (2003) 047002.

[8] M. Ivarone, G. Karapetrov, A.E. Koshelev, W.K. Kwok, G.W. Crabtree, D.G. Hinks, W.N. Kang, E.-M. Choi, H.J. Kim, H.J. Kim, S.I. Lee, Phys. Rev. Lett. 89 (2002) 187002.

[9] R. Gonnelli, D. Daghero, G.A. Ummarino, V.A. Stepanov, J. Jun, S.M. Kazakov, J. Karpinski, Phys. Rev. Lett. 89 (2002) 247004.

[10] M. Angst, R. Puzniak, A. Wisniewski, J. Jun, S.M. Kazakov, J. Karpinski, J. Roos, H. Keller, Phys. Rev. Lett. 88 (2002) 167004.

[11] V.G. Kogan, Phys. Rev. B 66 (2002) 020509;
V.G. Kogan, S.L. Bud'ko, Physica C 385 (2003) 131.

[12] J. Karpinski, M. Angst, J. Jun, S.M. Kazakov, R. Puzniak, A. Wisniewski, J. Roos, H. Keller, A. Perucci, L. Degiorgi, M.R. Eskildsen, P. Bordet, L. Vinnikov, A. Miranov, Supercond. Sci. Technol. 16 (2003) 221.

[13] F. Bouquet, Y. Wang, I. Sheikin, T. Plackowski, A. Junod, S. Lee, S. Tajima, Phys. Rev. Lett. 89 (2002) 257001.

[14] N. Nakai, P. Miranovic, M. Ichioka, K. Machida, Phys. Rev. Lett. 89 (2002) 237004.

[15] J. Kortus, private communication.

[16] L.J. Campbell, M.M. Doria, V.G. Kogan, Phys. Rev. B 38 (1988) 2439.